

# An animal model to study human muscular diseases involving mitochondrial oxidative phosphorylation

Hélène Lemieux · Blair E. Warren

Received: 10 May 2012 / Accepted: 30 May 2012 / Published online: 16 June 2012  
© Springer Science+Business Media, LLC 2012

**Abstract** Mitochondria are producing most of the energy needed for many cellular functions by a process named oxidative phosphorylation (OXPHOS). It is now well recognized that mitochondrial dysfunctions are involved in several pathologies or degenerative processes, including cardiovascular diseases, diabetes, and aging. Animal models are currently used to try to understand the role of mitochondria in human diseases but a major problem is that mitochondria from different species and tissues are variable in terms of regulation. Analysis of mitochondrial function in three species of planarian flatworms (*Tricladia*, *Platyhelminthes*) shows that they share a very rare characteristic with human mitochondria: a strong control of oxidative phosphorylation by the phosphorylation system. The ratio of coupled OXPHOS over maximal electron transport capacity after uncoupling (electron transport system; ETS) well below 1.0 indicates that the phosphorylation system is limiting the rate of OXPHOS. The OXPHOS/ETS ratios are  $0.62 \pm 0.06$  in *Dugesia tigrina*,  $0.63 \pm 0.05$  in *D. dorotocephala* and  $0.62 \pm 0.05$  in *Prococtyla fluviatilis*, comparable to the value measured in human muscles. To our knowledge, no other animal model displays this peculiarity. This new model offers a venue in which to test the phosphorylation system as a potential therapeutic control point within humans.

**Keywords** Animal model · Cardiovascular disease · Human muscular disease · Oxidative phosphorylation · Planarian · Phosphorylation system

## Abbreviations

Cyt. <i>c</i>	Cytochrome <i>c</i>
DNP	Dinitrophenol
ETS	Electron transport system
G3Pdh	Glycerol-3-phosphate dehydrogenase
IM	Isolated mitochondria
LA	Left atrium
LV	Left ventricle
PA	Permeabilized animal
PF	Permeabilized fibers
PM	Pyruvate and malate
RCR	Respiratory control ratio
ROX	Residual oxygen consumption
S(rot)	Succinate and rotenone
TMPD	Tetramethylphenylenediamine
V	Ventricle
WH	Whole heart
Ww	Wet weight

## Introduction

Up to now, hundreds of mitochondrial proteins have been implicated in human diseases (Chinault et al. 2009; Schwimmer et al. 2006). Unfortunately, even when the protein involved in the disease is identified, the mechanistic link between the protein dysfunction and the diseases remains often unclear (Rea et al. 2010). For close to 60 % of mitochondrial disorders, the causative factors have not been identified (Dimmer et al. 2002). Delineation of these causative factors is however critical since mitochondrial dysfunction have been tightly related to cardiovascular diseases (Lemieux and Hoppel 2009; Lemieux et al. 2011), diabetes (Anderson et al. 2009; Boushel et al. 2007), and aging (see reviews Lesnefsky and Hoppel 2006; Rosca et al. 2009a; among others).

H. Lemieux (✉) · B. E. Warren  
Campus Saint-Jean, University of Alberta,  
8406, Marie-Anne-Gaboury Street (91 Street),  
Edmonton, Alberta T6C 4G9, Canada  
e-mail: helene.lemieux@ualberta.ca

Mitochondria produce the major fraction of muscle energy via a process called oxidative phosphorylation (OXPHOS; Fig. 1). During this process, the electrons are transferred into the electron transport system (ETS), located in the mitochondrial inner membrane, while protons are pumped into the intermembrane space at the level of complexes I, III, and IV. The proton gradient formed between the two mitochondrial membranes is used by the phosphorylation system to produce energy in the form of ATP. The energy generated by oxidative phosphorylation depends not only on the efficiency of electron transport between the complexes I to IV of the ETS, but also on the ability of the phosphorylation system to convert the proton gradient into energy (Fig. 1).

The strides in understanding human muscular diseases have been driven largely by genetic approaches using model systems such as transgenic mice (Wallace 2002; Zaragoza et al. 2011). Animal models are useful to discern the roles of mitochondrial proteins in the etiology of disease involving mitochondria (Rea et al. 2010). These animal models should allow not only the identification of genes and proteins associated with the disease, but also to determine at which level energy production is impaired in the mitochondria. The regulation of OXPHOS should therefore be carefully scrutinized. Unfortunately, mitochondria are not functionally equivalent among different species and tissues, and the divergence in the OXPHOS regulation processes are rarely considered in studies performed with animal models.

A very peculiar property of mitochondria from human heart (Lemieux et al. 2011) and skeletal muscle (Boushel et al. 2007) is the strong control exerted by the phosphorylation system on OXPHOS. Because the main purpose of

OXPHOS is to produce energy, the control of OXPHOS by the phosphorylation system is of major consequence for muscle contraction. To measure the limitation of OXPHOS by the phosphorylation system in permeabilized tissues or isolated mitochondria, an uncoupler is added to the mitochondria respiring in the presence of excess substrates and ADP. The addition of the uncoupler allows the protons to come back through the mitochondrial membrane without passing through the ATP synthase (Fig. 1). The contribution of the phosphorylation system in the regulation of oxidative phosphorylation is quantified by the ratio of coupled OXPHOS over maximal electron transport capacity after uncoupling (ETS; Pesta and Gnaiger 2011). A ratio of 1.0 indicates that the capacity of the phosphorylation system is enough to support the capacity of electron transfer in the ETS, and that the control of OXPHOS is at the level of the ETS (Pesta and Gnaiger 2011). A ratio below 1.0 indicates that the phosphorylation system is limiting the rate of OXPHOS. In a healthy human heart, the OXPHOS/ETS ratio is 0.48, indicating that OXPHOS capacity is dictated by the phosphorylation system which can support less than 50 % of the ETS capacity (Lemieux et al. 2011; Table 1). In human skeletal muscle, the ratio is around 0.8, showing that the phosphorylation system capacity is 20 % lower than the ETS capacity (see Table 1 for references).

Heart and skeletal muscle from currently used mammal models such as rat and mouse do not present such a limitation of OXPHOS by the phosphorylation system (Aragonés et al. 2008; Hickey et al. 2009; Lemieux et al. 2010; see Table 1). In rodent muscles where the capacity of the phosphorylation system can support the maximum proton flux

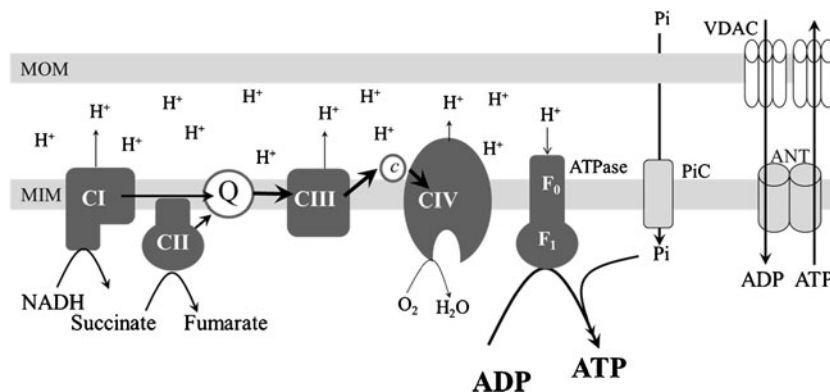


**Fig. 1** Scheme of oxidative phosphorylation (OXPHOS) in mitochondria. The electron transport system (ETS) located in the mitochondrial inner membrane (MIM) includes the complexes I (CI), II (CII), III (CIII), and IV (CIV). The electrons enter into the ETS via CI, CII, electron transferring flavoprotein, and glycerophosphate dehydrogenase (later two are not shown). Substrates for CI provide electrons from NADH via the citric acid cycle. Succinate provides FADH<sub>2</sub> feeding electrons into CII. Electrons from CI and CII converge at the Q-cycle before going to CIII and CIV. When electrons are transferred into the ETS, protons are pumped into the intermembrane space at the

level of CI, CIII, and CIV. The proton gradient is used by the phosphorylation system to produce energy in the form of ATP. The phosphorylation system is composed of the ATP synthase, the adenine nucleotide translocase (ANT), and the phosphate carrier (PiC). ADP enters the mitochondrial outer membrane (MOM) through voltage-dependent anion channel (VDAC) and the MIM through the adenine nucleotide translocase (ANT). The phosphate freely passes through the MOM and is transported through the MIM via the PiC. The ATP synthase uses the phosphate and the ADP to make ATP

**Table 1** OXPHOS/ETS ratios in the animal kingdom

Tissues	Species	Complexes	OXPHOS/ETS ratios	References
<b>Heart</b>				
LA (PF)	Human (control donors)	I	0.48	(Lemieux et al. 2011)
		II	0.92	(Lemieux et al. 2011)
LV (IM)	Pig	I	0.97	(Mootha et al. 1997)
LV (IM)	Dog	I	0.96	(Mootha et al. 1997)
LV (IM)		I	0.98–0.99	(Rosca et al. 2008)
LV (PF)	Rat	I+II	1.0	(Hickey et al. 2009; Lemieux et al. 2010)
WH (IM)		I	0.98	(Chen et al. 2008)
		II	0.97	(Chen et al. 2008)
LV (PF)	Mouse	I+II	1.0	(Lemieux et al. 2006)
V (IM)	Mouse	II	1.0	(ter Veld et al. 2005)
V (PF)	Fish <i>Forsterygion varium</i> , <i>F. malcolmi</i> , <i>Bellapiscis medius</i>	I+II	0.95–1.0	(Hilton et al. 2010)
V (PF)	Epaulette shark <i>Hemiscyllium ocellatum</i> , <i>Solvenose ray</i> <i>Aptychotrema rostrata</i>	I+II	0.59–0.77	(Hickey et al. 2012)
<b>Skeletal muscle</b>				
Quadriceps (IM)	Human	I+II	0.69–0.72	(Rasmussen and Rasmussen 2000) (Rasmussen et al. 2001)
		I	0.80–0.86	(Rasmussen and Rasmussen 2000)
		II	0.93	(Rasmussen and Rasmussen 2000)
Vastus lateralis (PF)	Human	I+II	0.79	(Boushel et al. 2007)
Triceps brachii (PM)	Horse	I+II (GMS)	0.67–0.91	(Votion et al. 2010; Votion et al. 2012)
Gastrocnemius (IM)	Dog	I	0.92–0.95	(Rosca et al. 2009b)
		II	1.0	(Rosca et al. 2009b)
Plantaris (PF)	Rat	I+II	1.0	(Wüst et al. 2012)
Soleus (PF)	Mouse	I+II	1.0	(Aragonés et al. 2008)
Gastrocnemius (IM)	Mouse	II	1.0	(ter Veld et al. 2005)
<b>Whole animal</b>				
(PA)	Brown planaria, <i>Dugesia tigrina</i>	I+II ( $n=10$ )	$0.62\pm 0.06$	Our results
		I ( $n=7$ )	$0.69\pm 0.05$	Our results
		II ( $n=9$ )	$0.86\pm 0.08$	Our results
(PA)	Black planaria, <i>D. dorotocephala</i>	I+II ( $n=4$ )	$0.63\pm 0.03$	Our results
(PA)	White planaria, <i>Procotyla fluviatilis</i>	I+II ( $n=5$ )	$0.62\pm 0.05$	Our results
(IM)	<i>C.elegans</i> (wild type)	I	0.95–1.0	(Kayser et al. 2001; Kayser et al. 2004)
(PA)	<i>Daphnia magna</i>	I+II ( $n=4$ )	$1.00\pm 0.01$	Our results
(PA)	<i>Drosophila simulans</i>	I+II+G3Pdh	0.97–0.99	(Pichaud et al. 2012)

LV Left ventricle; V Ventricle; IM Isolated mitochondria; PF Permeabilized fibers; PA Permeabilized animal; G3Pdh Glycerol-3-phosphate dehydrogenase; WH Whole heart; LF Left atrium

generated by the electron transport in the ETS, a disease affecting an ETS complex will have major consequences on energy production. In contrast, in human muscles where the ETS capacity exceed the proton flux that can be supported by the phosphorylation system, a decrease in electron transport through the ETS will not immediately affect energy production. However, with human muscles, any defect in the

phosphorylation system components (Fig. 1) could have major consequences. As an example, decreases in the capacity of the phosphorylation system have been measured early in the development of human heart failure, and contribute to the loss of energy production by the heart (Lemieux et al. 2011).

Finding an animal model that displays the particular characteristics of human mitochondria is essential for

exploring how mitochondrial dysfunction can lead to general metabolic impairment and human diseases. The major mechanism of regulation of OXPHOS should correspond to the one observed in human muscles: a strong control by the phosphorylation system. Such a model will be of major interest, for example, in finding pharmaceutical compounds that act directly upon the regulation of OXPHOS. Worms are widely used animal models and are currently used for studying aging (Sedensky and Morgan 2006) and diseases involving mitochondria (Rea et al. 2010). Here we highlight the planarian flatworms (order Tricladida, class Turbellaria, phylum Platyhelminthes), as a new model to study human diseases affecting skeletal muscle and cardiac mitochondria.

## Methods

### Animals

Brown planaria (*Dugesia tigrina*), Black planaria (*D. dorocephala*), and White planaria (*Proclotyla fluviatilis*) are obtained from Ward's Natural Science Canada (St. Catharines, ON, Canada) and were maintained at room temperature in a modified zooplankton medium (Lynch et al. 1986) containing (concentrations in  $\text{mg}\cdot\text{l}^{-1}$ , if not otherwise specified): KCl (50),  $\text{MgSO}_4$  (40),  $\text{CaCl}_2$  (26.5),  $\text{K}_2\text{HPO}_4$  (6),  $\text{KH}_2\text{PO}_4$  (6),  $\text{NaNO}_3$  (50),  $\text{NaSiO}_3$  (20),  $\text{FeCl}_3$  (1.1), and preconditioned water from a gold fish tank ( $100\text{ ml}\cdot\text{l}^{-1}$ ). *D. tigrina* and *D. dorocephala* were fed once a week with beef liver. *Daphnia magna* were cultured in the same zooplankton medium without  $\text{NaSiO}_3$  and were fed 2–3 times a week with the algae *Chlamydomonas sp.* Care of the animals was approved by the animal care and use committee (Biosciences) of the University of Alberta.

### Animal permeabilization and high-resolution respirometry

Each planarian was weighed and used fresh for high-resolution respirometry measurement. The animal was rinsed twice with 0.5 ml of ice-cold relaxing solution containing 2.77 mM  $\text{CaK}_2\text{EGTA}$ , 7.23 mM  $\text{K}_2\text{EGTA}$ , 20 mM imidazole, 20 mM taurine, 6.56 mM  $\text{MgCl}_2$ , 5.77 mM ATP, 15 mM phosphocreatine, 0.5 mM dithiothreitol, 50 mM K-MES (pH 7.1 at 0 °C). After careful permeabilization with small forceps, the animal was agitated for 30 min at 4 °C in the relaxing solution supplemented with  $50\ \mu\text{g}\cdot\text{ml}^{-1}$  saponin (Kuznetsov et al. 2004; Veksler et al. 1987). The tissue was immediately transferred into the respiration chamber (OROBOROS Oxygraph 2 k, Innsbruck, Austria) containing 2 ml of respiration medium Mir05 (110 mM sucrose, 60 mM K-lactobionate, 0.5 mM EGTA,  $1\ \text{g}\cdot\text{l}^{-1}$  BSA fatty acid free, 3 mM  $\text{MgCl}_2$ , 20 mM taurine, 10 mM  $\text{KH}_2\text{PO}_4$ , 20 mM K-HEPES, pH 7.1; Gnaiger et al.

2000). The same method was applied for *D. magna*, except that the weight was not measured. In each respiration chamber, one *D. tigrina* or *D. dorocephala*, 3 to 4 *P. fluviatilis*, and 10–20 *D. magna* were used. Respiration was measured at 20 °C. Datlab software (OROBOROS Instruments) was used for data acquisition and analysis.

The protocols for evaluating mitochondrial function are presented in Fig. 2a, b, and c. The final concentration of substrates, the uncoupler, and inhibitors added to the chambers were: pyruvate 5 mM, malate 5 mM, ADP 2.5 mM, cytochrome *c* (cyt. *c*) 10  $\mu\text{M}$ , succinate 10 mM, dinitrophenol (DNP) titration up to an optimum concentration of 80–180  $\mu\text{M}$  for planarians and 25  $\mu\text{M}$  for *D. magna*, rotenone 0.5  $\mu\text{M}$ , antimycin A 2.5  $\mu\text{M}$ , ascorbate 2 mM, tetramethylphenylenediamine (TMPD) 0.5 mM, azide 15 mM. Mitochondrial respiration was corrected for oxygen flux due to instrumental background, and for residual oxygen consumption (ROX) after inhibition of complexes I and III with rotenone and antimycin A. For complex IV respiration (ascorbate + TMPD), the chemical background measured in the presence of azide was subtracted. Respiratory flux in planarians is expressed in  $\text{pmol}\ \text{O}_2$  per second per mg wet weight (ww).

### Data analysis

Statistical analyses were performed using SigmaStat 4 (Aspire Software International, Ashburn, VA). A *t*-test for dependent samples was used to determine the effects of the additions of cytochrome *c* and uncoupler.  $P < 0.05$  was considered significant. Results are presented as means  $\pm$  standard deviation.

## Results

### Pattern of mitochondrial respiration in *D. tigrina*

In the protocol A (Figs 2a and 3a), resting respiration (LEAK) is measured in the presence of pyruvate + malate, before the addition of ADP. LEAK respiration is the oxygen consumption that represents proton leak, electron slip, and proton cycling (Brand et al. 1994). In permeabilized *D. tigrina*, LEAK respiration is low ( $0.53 \pm 0.41\ \text{pmol}\ \text{s}^{-1}\ \text{mg}^{-1}\ \text{ww}$ ) compared to respiration coupled with the production of ATP (OXPHOS;  $4.08 \pm 0.78\ \text{pmol}\ \text{s}^{-1}\ \text{mg}^{-1}\ \text{ww}$ ). The respiratory control ratio (RCR; OXPHOS/LEAK) of  $16.27 \pm 16.69$  reflects the high coupling of mitochondrial respiration, a first indication of good mitochondrial quality. The integrity of the outer mitochondrial membrane in the permeabilized animal is shown by the addition of exogenous cytochrome *c* (Fig. 2a), leading to only a small increase of OXPHOS ( $12.45 \pm 3.24\ \%$ ). Addition of succinate to complex I substrates increases OXPHOS

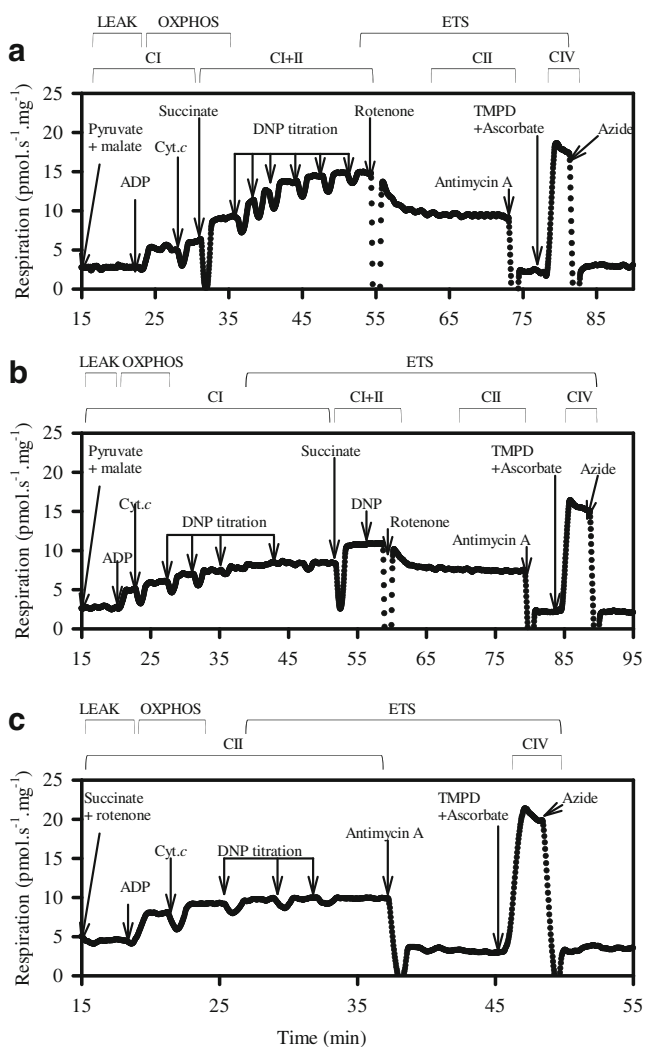


**Fig. 2** Limitation of oxidative phosphorylation (OXPHOS) by the phosphorylation system measured in permeabilized *Dugesia tigrina* in the presence of complexes I+II (CI+II) substrates (titration protocol A), complex I (CI) substrates (titration protocol B), and the complex II (CII) substrate (titration protocol C). The traces show typical experiments and represent the oxygen consumption as a function of time. Arrows indicate times of titrations of the substrates, uncoupler, and inhibitors. The first protocol (A) comprised the following steps: resting respiration (without ADP, LEAK) in the presence of CI substrates pyruvate+malate (PM); coupled respiration (OXPHOS) in the presence of PM and saturating ADP; integrity of the mitochondrial outer membrane measured with addition of cytochrome c; maximal OXPHOS with CI+II substrates after addition of succinate to CI substrates; maximal electron transport system (ETS, CI+II) capacity after uncoupling with dinitrophenol (DNP); CII ETS capacity after inhibition of CI with rotenone; residual oxygen consumption after inhibition of complex III with antimycin A; complex IV (CIV) respiration in the presence of ascorbate+TMPD (AsTm); inhibition of complex IV with azide. In the second protocol (B) the titration with DNP is performed in the presence of CI substrates (PM) only. The addition of succinate after the DNP measures CI+II ETS capacity. A second addition of DNP insures the full uncoupling in the presence of CI+II substrates simultaneously. In the third protocol (C) the titration with DNP is performed in the presence of the CII substrate (succinate+rotenone)

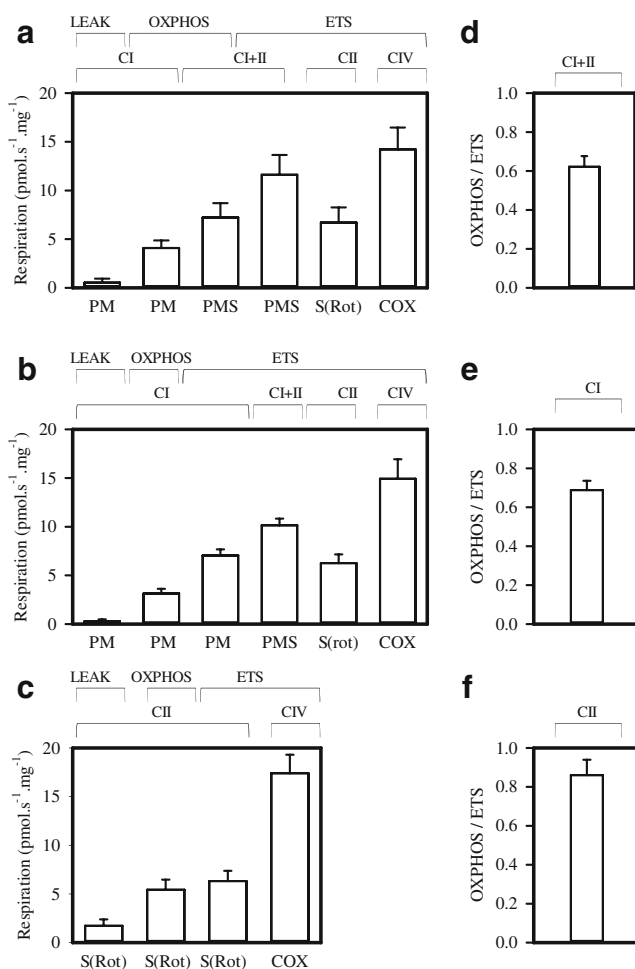


**Fig. 3** Mitochondrial respiration in permeabilized *D. tigrina* with the three multiple titration protocols. See Fig. 2 for abbreviations. A, B, and C represents the mitochondrial respiration in  $\text{pmol.s}^{-1}.\text{mg}^{-1}$  wet weight measured with the three protocols (Fig. 2). The OXPHOS/ETS coupling control ratios are measured with substrates for complexes I+II (D, protocol A), for complex I (E, protocol B), and for complex II (F, protocol C). Data are means $\pm$ SD.  $N=10, 7, 9$  for protocols A, B, and C respectively

by 1.8-fold, leading to an oxygen consumption of  $7.23 \pm 1.46 \text{ pmol s}^{-1} \text{ mg}^{-1} \text{ ww}$  in the presence of substrates that feed electrons into complexes I + II simultaneously (Figs. 2a and 3a). Uncoupling with DNP further increases complexes I + II respiration and gives the maximal ETS capacity ( $11.61 \pm 2.03 \text{ pmol s}^{-1} \text{ mg}^{-1} \text{ ww}$ ; Figs. 2a and 3a). Addition of rotenone inhibits complex I and isolates the respiration due to the entry of electrons through complex II [S(Rot):  $6.69 \pm 1.56 \text{ pmol s}^{-1} \text{ mg}^{-1} \text{ ww}$ ; Figs. 2a and 3a]. After inhibition of complex III with antimycin A, ascorbate and TMPD are added to measure the respiration of complex IV (cytochrome c oxidase, COX;  $14.22 \pm 2.24 \text{ pmol s}^{-1} \text{ mg}^{-1} \text{ ww}$ ; Figs. 2a and 3a).

In the protocol B (Figs. 2b and 3b), the respiration rate for LEAK and OXPHOS in the presence of complex I

substrates (pyruvate + malate) is not significantly different from the rates obtained in protocol A. Uncoupling with DNP further increases respiration, giving a complex I ETS capacity of  $7.05 \pm 0.61 \text{ pmol s}^{-1} \text{ mg}^{-1} \text{ ww}$  (Figs. 2b and 3b). Addition of succinate to complex I substrates further increases respiration by 1.4-fold (complexes I + II ETS;  $10.21 \pm 1.08 \text{ pmol s}^{-1} \text{ mg}^{-1} \text{ ww}$ ; Figs. 2b and 3b). The maximal ETS capacity with complexes I + II substrates did not show any significant differences between protocols A and B (Figs. 3 a, b).

In the protocol C (Figs. 2c and 3c), LEAK respiration in the presence of the complex II substrate (succinate + rotenone) is higher ( $1.73 \pm 0.66 \text{ pmol s}^{-1} \text{ mg}^{-1} \text{ ww}$ ; Fig. 3c) compared to LEAK respiration in the presence of the complex I substrates (Figs. 3a, b). OXPHOS in the presence of succinate + rotenone reaches  $5.43 \pm 1.04 \text{ pmol s}^{-1} \text{ mg}^{-1} \text{ ww}$  (Fig. 3c). Uncoupling with DNP further increases respiration to a complex II ETS capacity of  $6.32 \pm 1.06 \text{ pmol s}^{-1} \text{ mg}^{-1} \text{ ww}$  (Fig. 3c). The values for ETS capacities of complexes II and IV do not significantly differ between the three protocols (Fig. 3a, b, and c).

Quality of the mitochondria is also evaluated with the coupling control ratio. LEAK respiration normalized for ETS capacity (LEAK/ETS ratio) provides an expression of coupling independent of any limitation by the phosphorylation system (Gnaiger 2009; Pesta and Gnaiger 2011). The ETS capacity is measured in the presence of (1) optimal uncoupler concentration to release the control of OXPHOS from the phosphorylation system and (2) complexes I + II substrates simultaneously. This ratio is  $0.04 \pm 0.03$  for protocol A and  $0.03 \pm 0.02$  for protocol B, indicating that mitochondria are well coupled.

#### Flux control ratios

The limitation of OXPHOS capacity by the phosphorylation system is expressed by the OXPHOS/ETS coupling control ratio. In *D. tigrina*, the ratio is measured in the presence of different substrates (Fig. 3d, e, f), with a careful titration of the uncoupling agent (DNP; Fig. 2). The titration is important because a small excess of uncoupler can exert a pronounced inhibitory effect (Gnaiger 2008; Steinlechner-Maran et al. 1996). The OXPHOS/ETS ratios in *D. tigrina* are  $0.62 \pm 0.06$  in the presence of complexes I + II substrates (Fig. 3d),  $0.69 \pm 0.05$  in the presence of complex I substrates only (Fig. 3e), and  $0.86 \pm 0.08$  in the presence of the complex II substrate (Fig. 3d, e, f, Table 1). The OXPHOS/ETS ratios are far from 1.00 which indicates that the phosphorylation system is limiting the OXPHOS capacity. In order to verify if our results were species specific, mitochondrial respiration is measured in two other species of planarian (*D. dorotocephala* and *Procotyla fluviatilis*) with the protocol A (Fig. 2a). OXPHOS/ETS ratios similar to the one

measured in *D. tigrina* were obtained for these two species (Table 1). In contrast, with *D. magna*, addition of an uncoupler does not affect the OXPHOS respiration, leading to an OXPHOS/ETS ratio of 1.0 (Table 1).

Leak respiration normalized for ETS capacity (LEAK/ETS) provides an expression of mitochondrial coupling that is independent of any limitation by the phosphorylation system (Gnaiger 2009). The low LEAK/ETS ratio in *D. tigrina* (0.03), compared to the ratio in well coupled human heart mitochondria (0.08–0.10), is indicative of the good quality of the mitochondrial preparation in the planarians.

#### Validation of the results obtained with *D. tigrina*

Control experiments are performed to exclude an ADP limitation and incomplete tissue permeabilization as factors responsible for the low OXPHOS/ETS ratio in *D. tigrina*. The first experiment (Fig. 4a) shows that complexes I + II OXPHOS capacity in the presence 2.5 mM ADP is not further stimulated by the addition of 1.25 mM ADP (final concentration 3.75 mM ADP). In the second experiment, creatine (10 mM) is added and does not exert an effect on OXPHOS (Fig. 4b), providing evidence that OXPHOS capacity is not limited by mitochondrial creatine kinase. Saponin ( $25 \text{ mg.ml}^{-1}$ ) is added to the O2k chamber to confirm complete permeabilization of the cell membrane. The saponin treatment causes a loss of mitochondrial coupling as the addition of ADP after saponin does not stimulate LEAK respiration (Fig. 4c). A large effect of cytochrome *c* is observed after saponin treatment in the chamber, indicating a loss of integrity of the outer mitochondrial membrane (Fig. 4c). Because the mitochondria are already uncoupled by the saponin treatment in the chamber, the addition of the uncoupler after cytochrome *c* does not stimulate respiration. The same results are obtained by the addition of digitonin into the chamber after the standard protocol for permeabilization of the animals (results not shown). A titration of saponin is performed in the O2k chamber after ADP stimulation. A gradual loss of OXPHOS capacity is observed after adding  $7.5 \text{ mg.ml}^{-1}$  saponin and a drastic loss after adding  $15 \text{ mg.ml}^{-1}$  of saponin. The OXPHOS capacity can be recovered by the addition of exogenous cytochrome *c*, showing the loss of integrity of the mitochondrial outer membrane (Fig. 4d). In the last test, the standard protocol of incubation of the permeabilized animal is performed with half of the saponin concentration used in the standard protocol (25 instead of  $50 \text{ mg.ml}^{-1}$ ). The results for OXPHOS (with cytochrome *c*  $4.72 \pm 0.62 \text{ pmol s}^{-1} \text{ mg}^{-1} \text{ ww}$ ) and ETS capacities (with pyruvate + malate + succinate:  $12.83 \pm 0.82 \text{ pmol.s}^{-1} \text{ mg}^{-1} \text{ ww}$ ) are similar to the results obtained with  $50 \text{ mg.ml}^{-1}$  of saponin ( $4.08 \pm 0.78$  and  $11.61 \pm 2.03 \text{ pmol.s}^{-1} \text{ mg}^{-1} \text{ ww}$ , respectively). The cytochrome *c* effect is not reduced when decreasing the

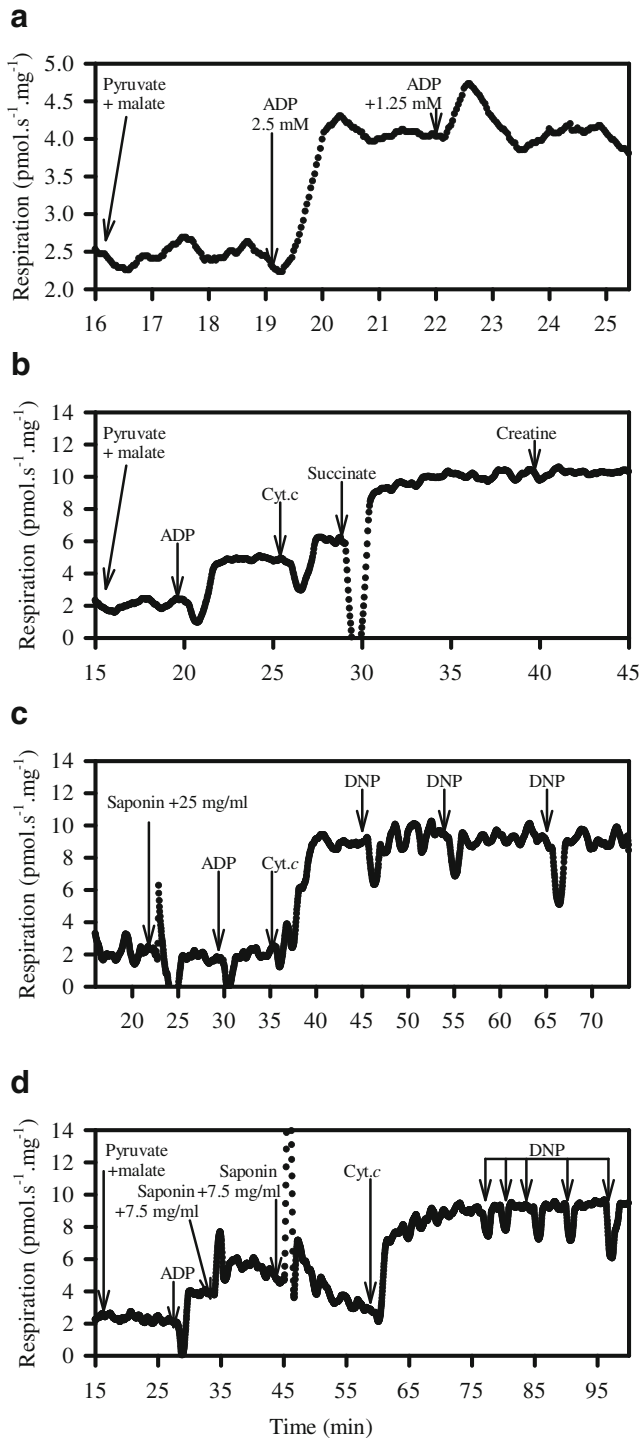


**Fig. 4** Validation of the results in *D. tigrina* by testing the ADP saturation and the full permeabilization. No stimulation of oxidative phosphorylation is observed by a second addition of ADP (a), or by addition of 10 mM creatine (b). Saponin added to the chamber at concentrations of 25 mg·ml<sup>-1</sup> (c) or 2-fold 7.5 mg·ml<sup>-1</sup> (d) increases dramatically the effect of cytochrome *c*

saponin concentration (19.33±0.36 % compared to 12.45±3.24 % with the protocol A).

## Discussion

The recognized link between mitochondrial dysfunction and human diseases has led to a growing interest for research in mitochondrial physiology. The very peculiar properties of human heart and skeletal muscle mitochondria have unfortunately not been taken into account in studies performed with animal models. Our results highlight the planarians as potential model species for mitochondrial oxidative phosphorylation. The planarians are, so far in the animal kingdom, the only species that can be used as an animal model and that share with human heart and skeletal muscle mitochondria a strong regulation of OXPHOS by the phosphorylation system.

The capacity of the phosphorylation system to use the proton gradient to produce ATP is a major determinant of the mitochondrial energy production in the three species of planarian included in our study. The limitation of OXPHOS by the phosphorylation system is shown by the increase in oxygen consumption after adding an uncoupling agent, which dissociates the transport of electrons into the ETS from the phosphorylation system. In *D. tigrina*, the limitation by the phosphorylation system is studied in the presence of substrates feeding electrons into complex I, into complex II, or into complexes I + II simultaneously. The convergent electron input from complexes I + II provides a maximum electron supply to the ETS and maximizes the limiting effect of the phosphorylation system under physiological conditions. The OXPHOS/ETS ratio in *D. tigrina* is 0.62 in the presence of complexes I + II substrates. This means that the ETS capacity is 61 % over the capacity of the phosphorylation system. In the presence of substrates feeding electrons only to complex I or II, the transfer of electrons into the ETS is not maximal, which leads to an underestimation of the limiting effect exerted by the phosphorylation system. Our results, however, show that even with single electron entry into the ETS, the ETS capacity is still 44 % over the phosphorylation capacity in the presence of complex I substrates (OXPHOS/ETS ratio of 0.69) and 16 % over in the presence of the complex II substrate (OXPHOS/ETS ratio of 0.86). The higher ratio in the presence of succinate is expected because complex II ETS capacity is lower compared to complex I ETS capacity. Furthermore, the P/O ratio is lower for complex II compared to complex I supported respiration, making a lower capacity of the phosphorylation system sufficient to match the oxygen consumption that is associated with complex II.

Similar OXPHOS/ETS ratios are obtained for two other species of planarians, *D. dorotocephala* and *P. fluviatilis* (Table 1). *D. dorotocephala* belongs to the same family (Planariidae) of planarians as *D. tigrina*. However, the similar ratio observed in *P. fluviatilis*, a species belonging to the Dendrocoelidae family, shows that this is a regulation

extended in the order of Tricladida. In the presence of complex I or complexes I + II substrates, planarian flatworm mitochondria show a limitation by the phosphorylation system that is similar to the human heart (0.48; Lemieux et al. 2011) and the human skeletal muscle (0.80; see references in Table 1). In the presence of the complex II substrate, the OXPHOS/ETS ratio is also similar to the human heart (0.92; Lemieux et al. 2008) and the human skeletal muscle (0.93; Rasmussen and Rasmussen 2000). In most other species of mammals, fish, and invertebrates, the OXPHOS is not limited by the phosphorylation system. In rat, mouse, pig, and dog heart and/or skeletal muscle mitochondria, the OXPHOS/ETS ratios are close to 1.0 (see Table 1). Furthermore, mitochondria from other interesting animal models such as nematodes (*Caenorhabditis elegans*), fruit flies (*Drosophila*), and cladocerans (*D. magna*) are not limited by the phosphorylation system (Table 1). Even though the mitochondria from horse skeletal muscle and from shark heart are limited by the phosphorylation system (Table 1), these animals are not practical models.

In order to make sure that the increased respiration in the presence of an uncoupler is indicative of a limitation by the phosphorylation system, we performed further tests in *D. tigrina*. ADP limitation and incomplete tissue permeabilization are two factors that could explain a low OXPHOS/ETS ratio without being from a true limitation of OXPHOS by the phosphorylation system. Addition of ADP or creatine do not stimulate OXPHOS, providing evidence that OXPHOS capacity is not limited by mitochondrial creatine kinase and ADP diffusion (Nascimben et al. 1996; Saks et al. 1991). Complete permeabilization of the cell membrane is confirmed by modification of the concentration of saponin or addition of digitonin. In case of partial mechanical and chemical permeabilization (Kuznetsov et al. 2002), one would expect an increase in OXPHOS with an increase in saponin concentration. However, the addition of saponin or digitonin into the oxygraph chamber causes a loss of mitochondrial coupling and a loss of integrity of the mitochondrial outer membrane. In contrast, a reduction of the saponin concentration did not affect the OXPHOS and ETS capacities, and did not improve the mitochondrial membrane integrity.

The limitation of OXPHOS by the phosphorylation system in planarians is not the only reason that makes it a good model for studying mitochondrial function. Planarians are small, easy, and cost-effective to culture in the laboratory (Gentile et al. 2011). Many species are available, which is an advantage in terms of genome diversity. Planarians share a significant amount of genes with humans, and a lot of these genes are related to diseases (review by Gentile et al. 2011). Most planarians show extraordinary developmental plasticity, including asexual and sexual modes of reproduction (Hoshi et al. 2003). Asexual reproduction of the planarians via transverse fission is one of the reasons why they are well

recognized as a suitable model for the study of regeneration processes. These animals have amazing regeneration capacity; a small fragment of this worm (1/279th) can regenerate into an entire animal, including the central nervous system (Newmark and Sánchez Alvarado 2002). The asexual reproduction allows generation of clonal lines with hundreds of thousands of fission progeny each week, all derived from a single individual (Newmark and Sánchez Alvarado 2002). This provides an exceptional opportunity to study responses to nutritional and pharmacological modulators, environmental stimuli, and toxins in a uniform genetic background with unlimited replication.

The ultimate objective when using animal models is to be able to translate the research to human applications. Only a third of the animal studies published in leading journals were successfully translated to the level of human randomized trials (Hackam and Redelmeier 2006). One of the potential reasons for the lack of correlation between human and animal studies is that the animal models do not necessarily reflect well the human environment. In our study, we highlight an animal model that mimics a unique property of human skeletal muscle and heart mitochondria, a strong limitation of OXPHOS by the phosphorylation system. This regulation of mitochondrial metabolism is very rare in the animal kingdom and is not observed in currently used animal models including those from mice and rats. With a regulation of oxidative phosphorylation similar to human muscles, planarians show tremendous potential as model species to understand the control of mitochondrial metabolism and its role in human diseases. It is also an ideal species for high-throughput screening for drug discovery in a whole-animal context. Such an animal model could allow the discovery of pharmaceutical products targeting directly the limiting step in energy production in humans, the phosphorylation system and its components.

**Acknowledgments** This study was supported by the four following grants to H. Lemieux: a discovery grant from the Natural Sciences and Engineering Research Council, a research grant and a startup grant from Campus Saint-Jean, and an equipment grant from the Canadian Foundation for Innovation. We are grateful to Pierre U. Blier for helpful comments on the manuscript and Patrick A. Drda for editorial review.

## References

- Anderson EJ, Kypson AP, Rodriguez E, Anderson CA, Lehr EJ, Neuffer PD (2009) Substrate-specific derangements in mitochondrial metabolism and redox balance in the atrium of the type 2 diabetic human heart. *J Am Coll Cardiol* 54:1891–1898
- Aragónés J, Schneider M, Van Geyte K, Fraisl P, Dresselaers T, Mazzone M, Dirckx R, Zacchigna S, Lemieux H, Nam Ho Jeoung NH, Lambrechts D, Bishop T, Lafuste P, Diez-Juan A, Harten SK, Van Noten P, De Bock K, Willam C, Tjwa M, Grosfeld A, Navet R, Moons L, Vandendriessche T, Deroose C, Wijeyekoon B,



- Nuyts J, Jordan B, Silasi-Mansat R, Lupu F, Dewerchin M, Pugh C, Salmon P, Mortelmans L, Gallez B, Gorus F, Buyse J, Sluse F, Harris RA, Gnaiger E, Hespel P, Van Hecke P, Schuit F, Van Veldhoven P, Ratcliffe P, Baes M, Maxwell P, Carmeliet P (2008) Deficiency or inhibition of oxygen sensor Phd1 induces hypoxia tolerance by reprogramming basal metabolism. *Nat Genet* 40:170–180
- Boushel R, Gnaiger E, Schjerling P, Skovbro M, Kraunsoe R, Flemming D (2007) Patients with type 2 diabetes have normal mitochondrial function in skeletal muscle. *Diabetologia* 50:790–796
- Brand MD, Chien LF, Ainscow EK, Rolfe DF, Porter RK (1994) The causes and functions of mitochondrial proton leak. *Biochim Biophys Acta* 1187:132–139
- Chen Q, Moghaddas S, Hoppel CL, Lesnfsky EJ (2008) Ischemic defects in the electron transport chain increase the production of reactive oxygen species from isolated rat heart mitochondria. *Am J Physiol Cell Physiol* 294:C460–C466
- Chinault AC, Shaw CA, Brundage EK, Tang LY, Wong LJ (2009) Application of dual-genome oligonucleotide array-based comparative genomic hybridization to the molecular diagnosis of mitochondrial DNA deletion and depletion syndromes. *Genet Med* 11:518–526
- Dimmer KS, Fritz S, Fuchs F, Messerschmitt M, Weinbach N, Neupert W, Westermann B (2002) Genetic basis of mitochondrial function and morphology in *Saccharomyces cerevisiae*. *Mol Biol Cell* 13:847–853
- Gentile L, Cebrià F, Bartscherer K (2011) The planarian flatworm: an in vivo model for stem cell biology and nervous system regeneration. *Dis Model Mech* 4:12–19
- Gnaiger E (2008) Polarographic oxygen sensors, the oxygraph and high-resolution respirometry to assess mitochondrial function. In: Dykens JA, Will Y (eds) *Mitochondrial dysfunction in drug-induced toxicity*. John Wiley, 327–352
- Gnaiger E (2009) Capacity of oxidative phosphorylation in human skeletal muscle. *New perspectives of mitochondrial physiology*. *Int J Biochem Cell Biol* 41:1837–1845
- Gnaiger E, Kuznetsov AV, Schneeberger S, Seiler R, Brandacher G, Steurer W, Margreiter R (2000) Mitochondria in the cold. In: Heldmaier G, Klingenspor M (eds) *Life in the cold*. Springer Berlin Heidelberg, New York, pp 431–442
- Hackam DG, Redelmeier DA (2006) Translation of research evidence from animals to humans. *JAMA* 296:1731–1732
- Hickey AJ, Chai CC, Choong SY, de Freitas Costa S, Skea GL, Phillips AR, Cooper GJ (2009) Impaired ATP turnover and ADP supply depress cardiac mitochondrial respiration and elevate superoxide in nonfailing spontaneously hypertensive rat hearts. *Am J Physiol Cell Physiol* 297:C766–C774
- Hickey AJ, Renshaw GM, Speers-Roesch B, Richards JG, Wang Y, Farrell AP, Brauner CJ (2012) A radical approach to beating hypoxia: depressed free radical release from heart fibres of the hypoxia-tolerant epaulette shark (*Hemiscyllium ocellatum*). *J Comp Physiol B* 182:91–100
- Hilton Z, Clements KD, Hickey AJ (2010) Temperature sensitivity of cardiac mitochondria in intertidal and subtidal triplefin fishes. *J Comp Physiol B* 180:979–990
- Hoshi M, Kobayashi K, Arioka S, Hase S, Matsumoto M (2003) Switch from asexual to sexual reproduction in the planarian *Dugesia ryukyuensis*. *Integr Comp Biol* 43:24224–24226
- Kayser EB, Morgan PG, Hoppel CL, Sedensky MM (2001) Mitochondrial expression and function of GAS-1 in *Caenorhabditis elegans*. *J Biol Chem* 276:20551–20558
- Kayser EB, Morgan PG, Sedensky MM (2004) Mitochondrial complex I function affects halothane sensitivity in *Caenorhabditis elegans*. *Anesthesiology* 101:365–372
- Kuznetsov AV, Schneeberger S, Seiler R, Brandacher G, Mark W, Steurer W, Saks V, Ussov Y, Margreiter R, Gnaiger E (2004) Mitochondrial defects and heterogeneous cytochrome *c* release after cardiac cold ischemia and reperfusion. *Am J Physiol-Heart Circul Physiol* 286:H1633–H1641
- Kuznetsov AV, Strobl D, Ruttman E, Königsrainer A, Margreiter R, Gnaiger E (2002) Evaluation of mitochondrial respiratory function in small biopsies of liver. *Anal Biochem* 305:186–194
- Lemieux H, Garedew A, Blier PU, Tardif J-C, Gnaiger E (2006) Temperature effects on the control and capacity of mitochondrial respiration in permeabilized fibers of the mouse heart. *Biochim Biophys Acta* 1757:201–202
- Lemieux H, Hoppel CL (2009) Mitochondria in the human heart. *J Bioenerg Biomembr* 41:99–106
- Lemieux H, Semsroth S, Antretter H, Höfer D, Gnaiger E (2011) Mitochondrial respiratory control and early defects of oxidative phosphorylation in the failing human heart. *Int J Biochem Cell Biol* 43:1729–1738
- Lemieux H, Semsroth S, Gnaiger E (2008) Respiratory control and mitochondrial defects in the failing human heart. *Biochim Biophys Acta* 1777:S80–S81
- Lemieux H, Vazquez EJ, Fujioka H, Hoppel CL (2010) Decrease in mitochondrial function in rat cardiac permeabilized fibers correlates with the aging phenotype. *J Gerontol A Biol Sci Med Sci* 65:1157–1164
- Lesnfsky EJ, Hoppel CL (2006) Oxidative phosphorylation and aging. *Ageing Res Rev* 5:402–433
- Lynch M, Weider LJ, Lampert W (1986) Measurement of the carbon balance in *Daphnia*. *Limnol Oceanogr* 31:17–33
- Mootha VK, Arai AE, Balaban RS (1997) Maximum oxidative phosphorylation capacity of the mammalian heart. *Am J Physiol-Heart Circul Physiol* 41:H769–H775
- Nascimben L, Ingwall JS, Pauletto P, Friedrich J, Gwathmey JK, Saks V, Pessina AC, Allen PD (1996) Creatine kinase system in failing and nonfailing human myocardium. *Circulation* 94:1894–1901
- Newmark PA, Sánchez Alvarado A (2002) Not your father's planarian: a classic model enters the era of functional genomics. *Nat Rev Genet* 3:210–219
- Pesta D, Gnaiger E (2011) High-resolution respirometry. OXPHOS protocols for human cell cultures and permeabilized fibres from small biopsies of human muscle. In: Palmeira C, Moreno A (eds) *Mitochondrial bioenergetics: methods and protocols*
- Pichaud N, Ballard JWO, Tanguay RM, Blier PU (2012) Naturally occurring mitochondrial DNA haplotypes exhibit metabolic differences: insight into functional properties of mitochondria. *Evolution*. doi:10.1111/j.1558-5646.2012.01683.x
- Rasmussen UF, Rasmussen HN (2000) Human quadriceps muscle mitochondria: a functional characterization. *Mol Cell Biochem* 208:37–44
- Rasmussen UF, Rasmussen HN, Krstrup P, Quistorff B, Saltin B, Bangsbo J (2001) Aerobic metabolism of human quadriceps muscle: in vivo data parallel measurements on isolated mitochondria. *Am J Physiol Endocrinol Metab* 280:E301–E307
- Rea SL, Graham BH, Nakamaru-Ogiso E, Kar A, Falk MJ (2010) Bacteria, yeast, worms, and flies: exploiting simple model organisms to investigate human mitochondrial diseases. *Dev Disabil Res Rev* 16:200–218
- Rosca MG, Lemieux H, Hoppel CL (2009a) Mitochondria in the elderly: is acetylcarnitine a rejuvenator? *Adv Drug Deliv Rev* 61:1332–1342
- Rosca MG, Okere IA, Sharma N, Stanley WC, Recchia FA, Hoppel CL (2009b) Altered expression of the adenine nucleotide translocase isoforms and decreased ATP synthase activity in skeletal muscle mitochondria in heart failure. *J Mol Cell Cardiol* 46:927–935
- Rosca MG, Vazquez EJ, Kerner J, Parland W, Chandler MP, Stanley W, Sabbah HN, Hoppel CL (2008) Cardiac mitochondria in heart failure: decrease in respirasomes and oxidative phosphorylation. *Cardiovasc Res* 80:30–39

- Saks VA, Belikova YO, Kuznetsov AV, Khuchua ZA, Branishte TH, Semenovskiy ML, Naumov VG (1991) Phosphocreatine pathway for energy transport: ADP diffusion and cardiomyopathy. *Am J Physiol* 261:30–38
- Schwimmer C, Rak M, Lefebvre-Legendre L, Duvezin-Caubet S, Plane G, di Rago JP (2006) Yeast models of human mitochondrial diseases: from molecular mechanisms to drug screening. *Biotechnol J* 1:270–281
- Sedensky MM, Morgan PG (2006) Mitochondrial respiration and reactive oxygen species in *C. elegans*. *Exp Gerontol* 41:957–967
- Steinlechner-Maran R, Eberl T, Kunc M, Margreiter R, Gnaiger E (1996) Oxygen dependence of respiration in coupled and uncoupled endothelial cells. *Am J Physiol Cell Physiol* 40: C2053–C2061
- ter Veld F, Jeneson JAL, Nicolay K (2005) Mitochondrial affinity for ADP is twofold lower in creatine kinase knock-out muscles—possible role in rescuing cellular energy homeostasis. *FEBS J* 272:956–965
- Veksler VI, Kuznetsov AV, Sharov VG, Kapelko VI, Saks VA (1987) Mitochondrial respiratory parameters in cardiac tissue: a novel method of assessment by using saponin-skinned fibers. *Biochim Biophys Acta* 892:191–196
- Votion D-M, Fraipont A, Goachet AG, Robert C, Van Erck E, Amory H, Ceusters J, La Rebière D, de Pouyade G, Franck T, Mouithys-Mickalad A, Niesten A, Serteyn D (2010) Alterations in mitochondrial respiratory function in response to endurance training and endurance racing. *Equine Vet J* 42:268–274
- Votion D-M, Gnaiger E, Lemieux H, Mouithys-Mickalad A, Serteyn D (2012) Physical fitness and mitochondrial respiratory capacity in horse skeletal muscle. *PLoS One* 7
- Wallace DC (2002) Animal models for mitochondrial disease. *Methods Mol Biol* 197:3–54
- Wüst RC, Myers DS, Stones R, Benoist D, Robinson PA, Boyle JP, Peers C, White E, Rossiter HB (2012) Regional skeletal muscle remodeling and mitochondrial dysfunction in right ventricular heart failure. *Am J Physiol Heart Circ Physiol* 302:H402–H411
- Zaragoza C, Gomez-Guerrero C, Martin-Ventura JL, Blanco-Colio L, Lavin B, Mallavia B, Tarin C, Mas S, Ortiz A, Egido J (2011) Animal models of cardiovascular diseases. *J Biomed Biotechnol*